N90-28281

SATELLITE-DERIVED CLOUD FIELDS DURING THE FIRE CIRRUS IFO CASE STUDY

Patrick W. Heck and Gary G. Gibson
Aerospace Technology Division, Planning Research Corporation
Hampton, Virginia 23666

Patrick Minnis and Edwin F. Harrison
Atmospheric Sciences Division, NASA Langley Research Center
Hampton, Virgina 23665-5229

1. Introduction

The First ISCCP Regional Experiment (FIRE) Cirrus Intensive Field Observation (IFO) program measured cirrus cloud properties with a variety of instruments from the surface, aircraft, and satellites. Surface and aircraft observations provide small-scale point and line measurements of different micro- and macrophysical properties of advecting and evolving cloud systems. Satellite radiance data may be used to measure the areal variations of the bulk cloud characteristics over meso- and large-scales. Ideally, the detailed cloud properties derived from the small-scale measurements should be tied to the bulk cloud properties typically derived from the satellite data. Full linkage of these data sets for a comprehensive description of a given cloud field, one of the goals of FIRE, should lead to significant progress in understanding, measuring, and modeling cirrus cloud systems. In this paper, the relationships derived from intercomparisons of lidar and satellite data by Minnis et al. (1989a) are exploited in a mesoscale analysis of the satellite data taken over Wisconsin during the Cirrus IFO Case Study.

2. Data and Methodology

Daytime half-hourly, 1-km visible (VIS, 0.65 μm) and 4x8-km infrared (IR, 11.5 μm) GOES data were used to construct bispectral histograms on a 0.5° latitude-longitude grid between 42°N and 47°N and 87°W and 92°W during 27-28 October 1986. The VIS data are stored as counts between 0 and 63 which were converted to radiance and reflectance, ρ. The IR data are stored as counts between 0 and 255 which are converted to equivalent blackbody temperature, T. Soundings taken every 6 hours over Green Bay, Wisconsin were used to determine the vertical variation of temperature. Linear interpolation between the soundings was used to estimate the temperatures at each half hour.

The parameters of interest here are cloud amount, C; cloud-top temperature, T_t; cloud-center temperature, T_c; cloud-top height, z_t; cloud-center height, z_c; cloud thickness, h; cloud emittance, ϵ; VIS optical depth, τ_v, and clear-sky temperature, T_{cs}. The relationships between these parameters during the IFO were explored by Minnis et al. (1989a,b) using combined satellite-lidar data. A simple physical model is used here to relate the observed reflectance to cloud optical depth:

$$\rho = T_a \chi_c \alpha_c + T_c T_u \rho_s + a_{sd}(1 - \alpha_d)(1 - T_c - \alpha_c). \qquad (1)$$

Cloud albedo is $\alpha_c = \alpha_c(\tau_v, \mu_0)$; the diffuse cloud albedo is $\alpha_d = \alpha_d(\tau_v)$; and the cloud anisotropic reflectance factor is χ_c. The values for the albedos are determined in the same manner as Minnis et al. (1989b) using the results of Takano and Liou (1989). Values for χ_c are taken from the results of Minnis et al. (1989a). Ozone transmittance above the cloud is T_a; T_c and T_u are the transmittances of the cloud to direct downward and upward VIS radiation, respectively; ρ_s is the clear-sky reflectance; α_{sd} is the diffuse clear-sky albedo; and μ_0 is the cosine of the solar zenith angle. The infrared optical depth is $\tau_e = 2.17\tau_v$. The effective infrared beam emittance is $\epsilon = 1 - \exp(-\tau_e / \mu)$, where μ is the cosine of the viewing zenith angle. Assuming a pixel is completely cloud-filled,

$$T_c = B^{-1}\{[B(T) - (1 - \epsilon)B(T_{cs})] / \epsilon\}. \qquad (2)$$

Details for computing T_t, z_c, z_t, and h are given in Minnis et al. (1989b).

The basic approach to deriving these parameters from a histogram is outlined below.

1) Consider all pixels with $T < T_{cs} - 3K$ as cloudy.
2) Assign pixel to altitude level: low, middle, or high (Fig. 1).
3) Compute average reflectance for each temperature in a layer.
4) Compute τ_v for each observed temperature within the layer.
5) Compute T_c, T_t, and ϵ for each observed T in the layer.
6) Compute average T_c, T_t, τ_v, and ϵ for each layer.
7) Compute z_c, z_t, and h for each layer from results of (6).
8) Compute mean values for each variable by combining layer reults.

The functions P_m and P_h describe the VIS-IR thresholds between low and middle and between middle and high cloud, respectively.

3. Results and Discussion

This approach was applied to the lidar-satellite data of Minnis et al. (1989a) to determine the errors in the resulting cloud parameters. A comparison of selected parameters for total cloudiness is shown in Fig. 2 for Fort McCoy data. Figure 3 shows the comparison of the lidar cloud-top heights and the satellite-derived high cloud-top altitudes. The comparison results are summarized in Table 1. The satellite-derived total cloud-center heights agree well with the lidar, on average, while the corresponding cloud-top altitudes are underestimated by 0.5 km. If only high clouds (as detected by the satellite) are considered, the satellite results agree with the lidar values of z_t, but underestimate the values of z_c. These differences may be attributed to several effects. Some midlevel cloudiness may have been within the satellite field of view and still not have advected over the lidar sites. Partially cloud-filled pixels may have decreased the altitudes of some pixels or the values of χ_c may have been inadequate at some hours.

Examples of the derived values of high and midlevel cloud fraction, z_c, and ϵ are shown in Figs. 4 - 7 for 15, 18, and 21 UTC during October 28, 1986. At 15 UTC, most of the clouds are above 6 km (Fig. 4). Midlevel cloudiness is confined to the southern portion of the region (Fig. 5). Average values of z_c range between 7 and 9 km (Fig. 6). The thicker clouds, as determined by the emittances, are primarily in the northern half of the IFO box (Fig. 7). By midday (18 UTC), an area of clearing has moved into central Wisconsin. Cloud-center heights have increased to 11 km in the east while some scattered high and midlevel clouds follow the clearing line. At 21 UTC, the average cloud heights vary from 7 to 9 km again with significant midlevel cloudiness in the northern half of the box. Some mesoscale structure is evident in the emittance fields.

4. Concluding Remarks

The cloud parameters derived with the empirical technique described represent the most accurate, detailed areal cloud properties available for the Case Study. Additional research using other IFO results with theoretical calculations is needed to generalize the technique used here.

REFERENCES

Minnis, P., J. M. Alvarez, D. F. Young, K. Sassen, and C. J. Grund, 1989a: Interpretation of cirrus cloud properties using coincident satellite and lidar data during the FIRE IFO. Presented at FIRE Annual Meeting/ASTEX Workshop, Monterrey, CA, July 10-14.

Minnis, P., P. W. Heck, and E. F. Harrison, 1989b: The 27-28 October 1986 FIRE Cirrus IFO case study: Cloud parameter fields derived from satellite data. Submitted to Mon. Wea. Rev.

Takano, Y. and K. N. Liou, 1989b: Radiative transfer in cirrus clouds: II. Theory and computation of multiple scattering in an anisotropic medium. J. Atmos. Sci., 46, 21-38.

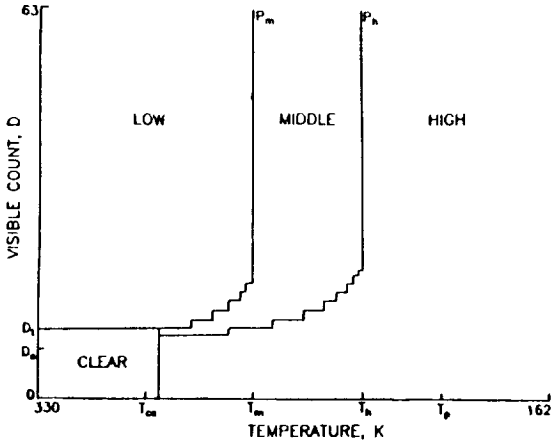

Fig. 1. Schematic diagram of histogram analysis.

Difference (Lidar - Satellite)	bias	rms
Total cloud		
z_c (km)	-0.08	0.94
z_t (km)	0.53	0.90
h (km)	0.29	1.00
ϵ	0.00	0.05
τ_v	-0.03	0.13
High clouds only		
z_c (km)	-0.41	1.13
z_t (km)	-0.09	0.63

Table 1. Differences between cloud parameter values derived with lidar-satellite data set and satellite data only.

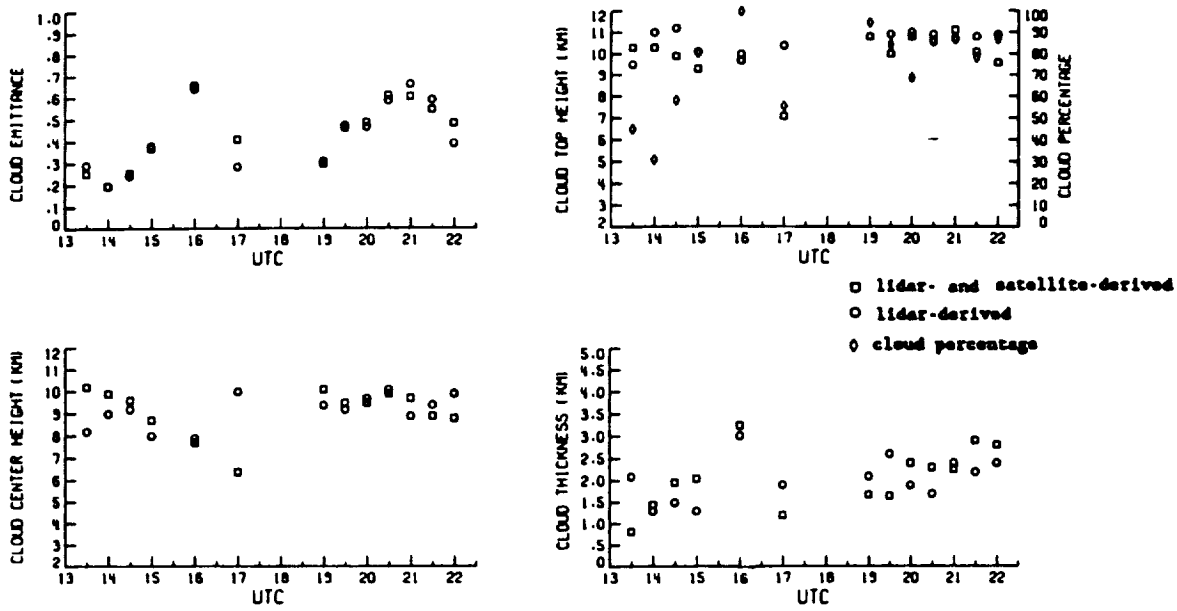

Fig. 2. Comparison of lidar and satellite-derived cloud parameters over Ft. McCoy, WI during October 28, 1986.

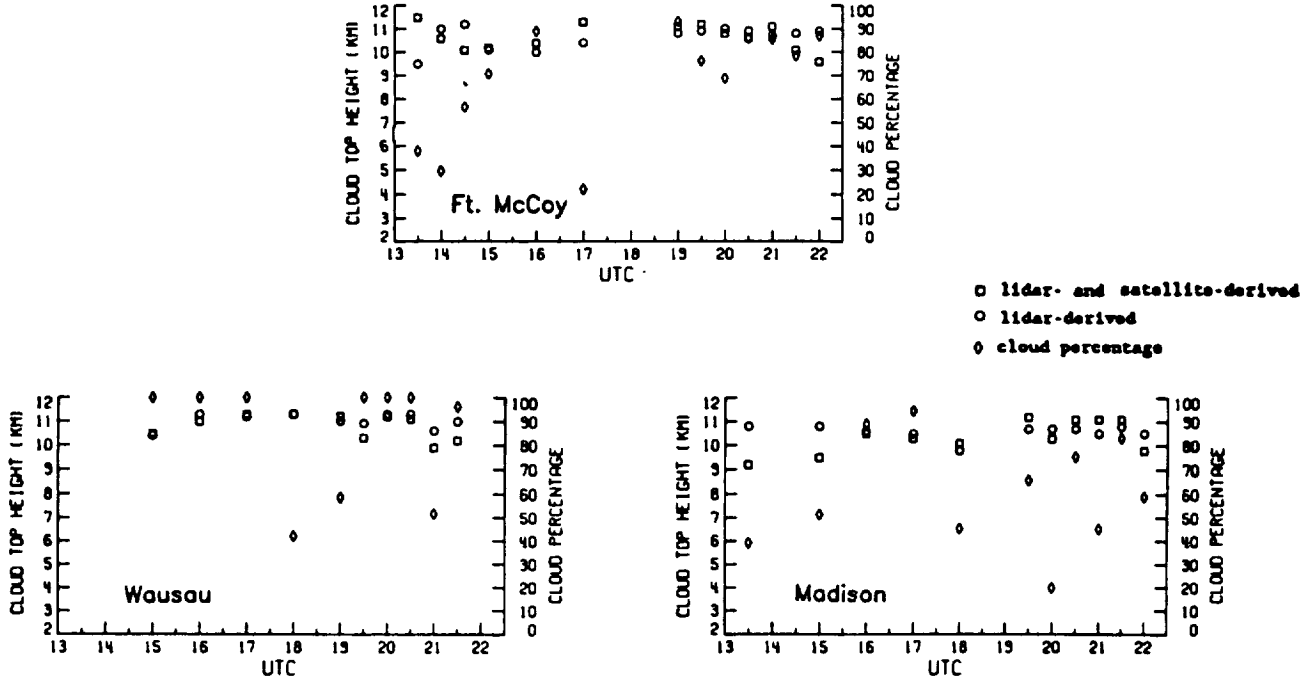

Fig. 3. Comparison of satellite-derived high cloud-top heights with lidar data for October 27-28, 1986.

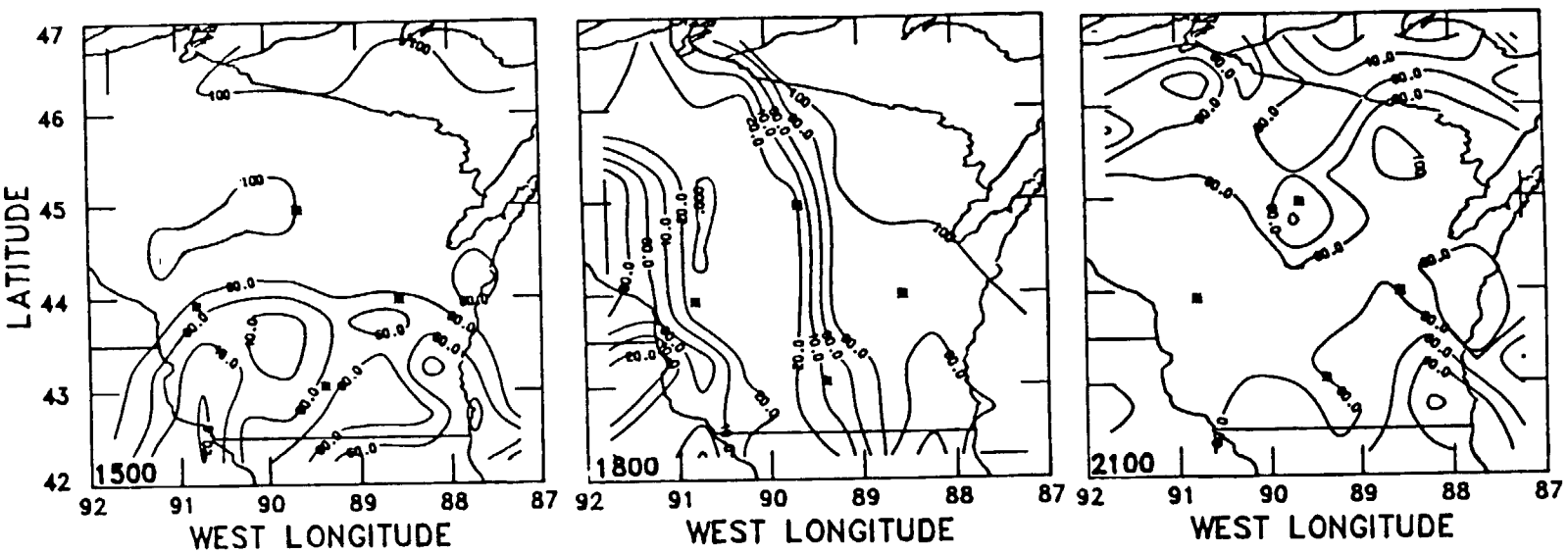

Fig. 4. GOES-derived high cloud amounts (%) for October 28, 1986.

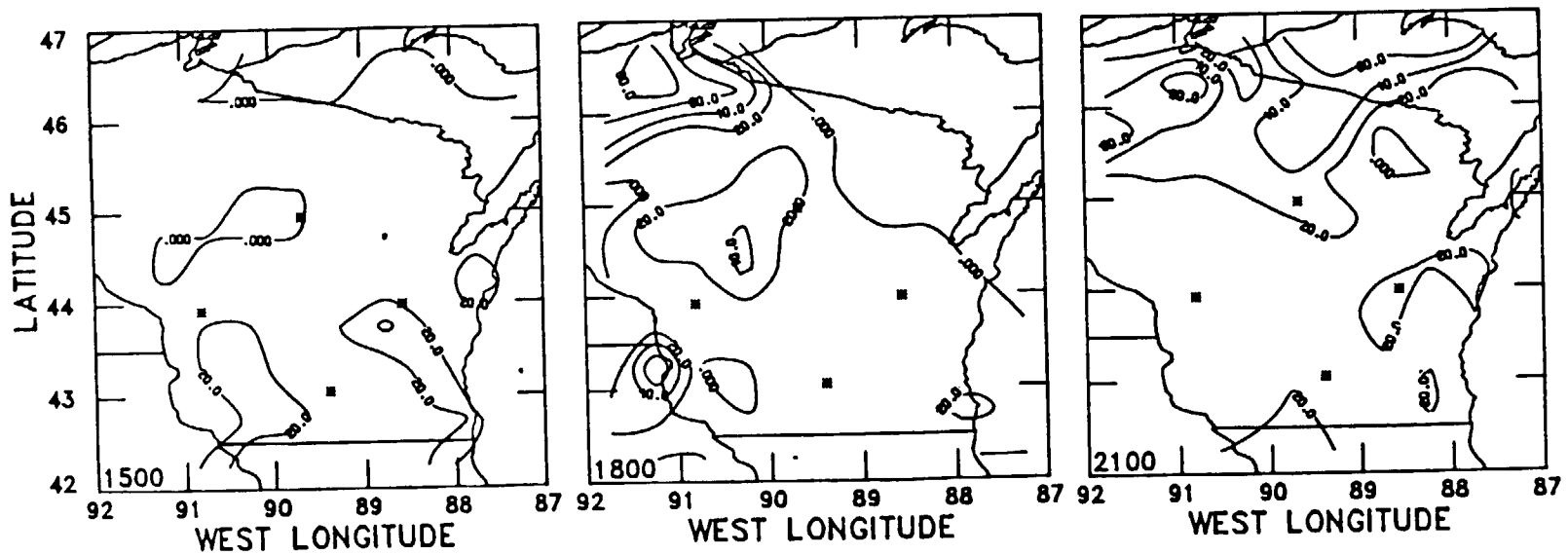

Fig. 5. GOES-derived midlevel cloud amounts (%) for October 28, 1986.

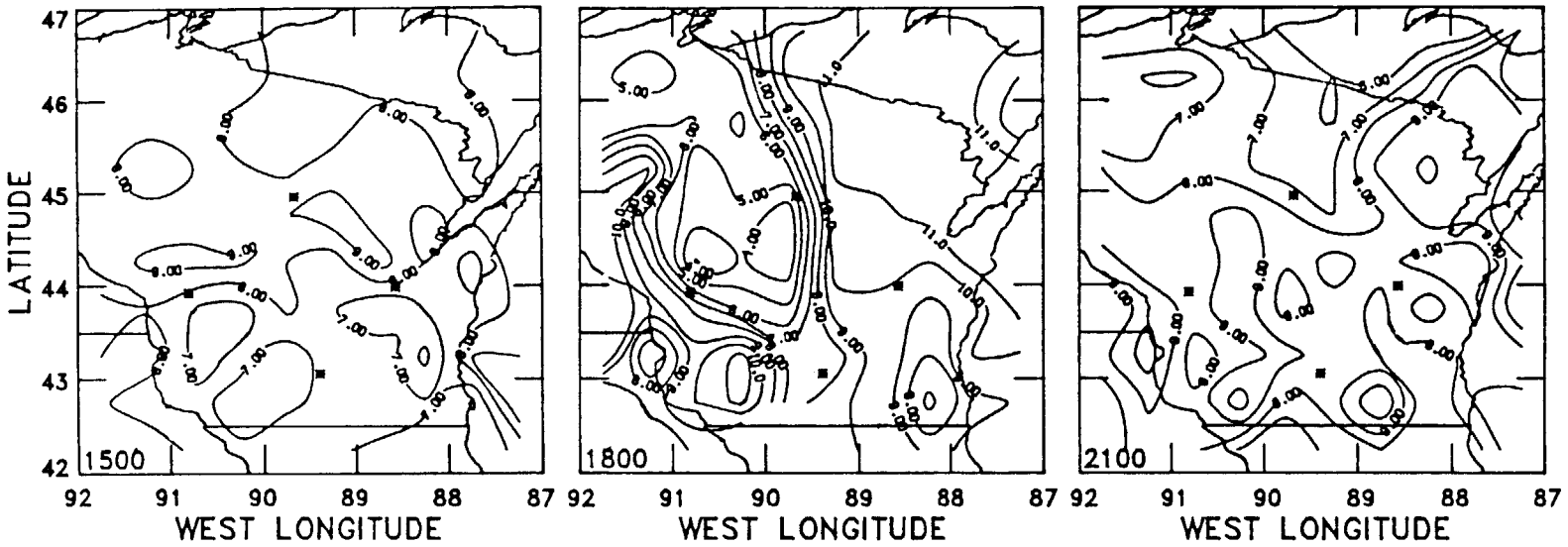

Fig. 6. GOES-derived cloud-center heights (km) for October 28, 1986.

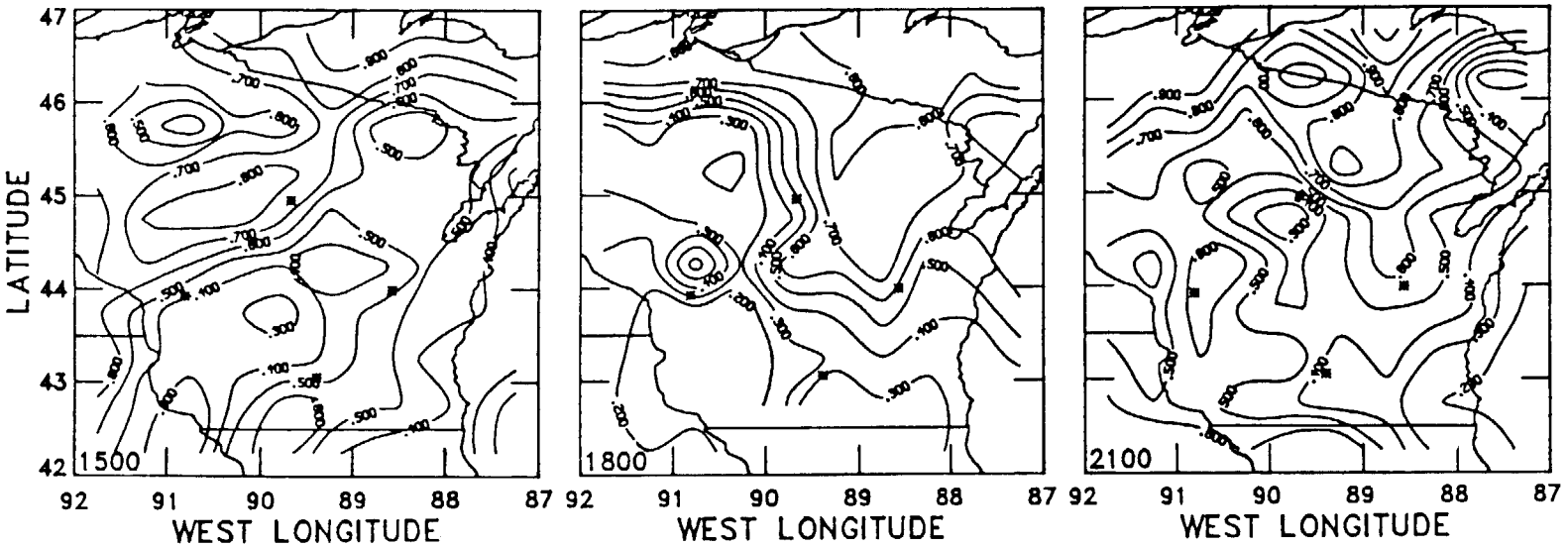

Fig. 7. GOES-derived cloud emittances for October 28, 1986.